AN EXPERIMENTAL STUDY ON SCALE EFFECTS IN SHEAR FAILURE OF REINFORCED CONCRETE COLUMNS

Takeshi OHTAKI[1]

SUMMARY

A shear dominated full-scale rectangular reinforced concrete column was tested under cyclic lateral loading. Two 1/2-scale units and three 1/4-scale units were designed to model the full-scale column as accurately as possible and tested using the same loading pattern as the full-scale column. Test variables also included the maximum aggregate size that was consistently scaled in accordance with the column size. The purpose of the test was to investigate the effect of scale on the shear behavior of reinforced concrete columns. The overall behaviors of the small-scale units were quite similar to the full-scale specimen during testing. The flexural and shear deformation components seemed to be consistently scaled and no scale effect was found. However, the shear crack inclination and the maximum crack width at an equivalent loading stage were different, which gave rise to the difference of the activation and the increasing rate of the transverse steel shear-resisting mechanisms V_s and consequently the difference of the degradation of the concrete shear-resisting mechanisms V_c. The concrete shear contribution computed from the applied lateral load and the measured hoop strains showed the scale effect in its maximum value for the test units with both constant and proportional aggregate size. On the other hand, though the V_c component at the maximum column strength decreased as the column size increased when the constant aggregate size was applied, no size effect was observed for the test units with proportional aggregate size. Design equations incorporating a scale factor seemed to appropriately estimate the concrete shear contribution, while that without size effect might be unconservative for large size columns.

INTRODUCTION

Seismic performance of reinforced concrete members is often studied using small-scale models because of constraints on economics, time, and laboratory space. However, the test results of small-scale models do not necessarily represent the behavior of full-scale structure. Therefore, it is essential to study the scale effect in order to employ the model test results to predict the behavior of full-scale structures.

Experimental evidence of size effect on shear strength of reinforced concrete members has been shown by many researchers [Kani 1967; Taylor 1972; Iguro 1984] and it is said that the effect of size is small for the beams with web reinforcement [ASCE-ACI 1973]. Also a number of theoretical approaches have been attempted to explain scale effect such as Bazant's size effect law [Bazant 1997] and Collins' modified compression field theory [Collins 1995]. However, most of the research works have been focused on the behavior of reinforced concrete beams without web reinforcement. Few relevant experimental data are available for large-scale reinforced concrete columns [Ohtaki 1996] and it was reported that no significant scale effect was found for circular reinforced columns [McDaniel 1997].

The shear behavior of structures depends on many variables including aspect ratio, longitudinal and transverse reinforcement ratio and cross section geometry, hence further research is necessary for a complete understanding of scale effect on shear behavior of reinforced concrete columns. In order to investigate the scale effects on the shear behavior, one shear dominated full-scale rectangular reinforced concrete column and two 1/2-scale models and three 1/4-scale models were tested under cyclic lateral loading.

[1] *Institute of Technology, Tokyu Construction Co., Ltd. Japan Email: t_ootaki@hd.tokyu-cnst.co.jp*

TEST UNITS AND SETUP

Test unit details

The details of the test units and the measured material properties are shown in Table 1. A full-scale rectangular reinforced concrete column was designed expecting shear failure. The column cross section was 2.0m×2.0m and the aspect ratio was 2.5. The longitudinal reinforcement consisted of 36-D51 (SD345) bars with a cover of 80mm. The transverse reinforcement consisted of D16 (SD295) rectangular hoops at a spacing of 300mm. The longitudinal and transverse reinforcement ratios were 1.82% and 0.07% respectively. The target compressive strength of concrete was 30 MPa. The small-scale units RM and RS series were designed as close to 1/2 and 1/4 the scale of unit RL-20 as possible. Special consideration was given to the transverse steel shear contribution to be equivalent between the test units, having equal product of yield strength and transverse reinforcement ratio, $f_{yh}\rho_v$. The scale of the maximum aggregate size was also taken into account as shown in the unit name in which number denoted the maximum aggregate size in mm. The reinforcement details of the test units are shown in Figure 1.

Table 1 Test Column Details

Unit	cross section	shear span	concrete compressive strength	maximum aggregate size	longitudinal reinforcement				transverse reinforcement			
	B Ð (mm)	*a (mm)*	*f'c (MPa)*	*ag (mm)*	*quantity*	*f Ïl (%)*	*yield strength fyl (MPa)*	*Young's modulus (GPa)*	*quantity*	*f Ïv (%)*	*yield strength fyh (MPa)*	*Young's modulus (GPa)*
RL-20	2000x2000	5000	29.7	20	36-D51	1.82	390	191	D16-@300	0.07	371	194
RM-20	1000x1000	2500	30.9	20	36-D25	1.82	376	193	D10-@210	0.07	363	185
RM-10			32.1	10								
RS-20	500x500	1250	43.1	20	36-D13	1.82	373	189	R4-@87	0.06	425	199
RS-10			48.4	10								
RS-05			35.3	5			360	194				

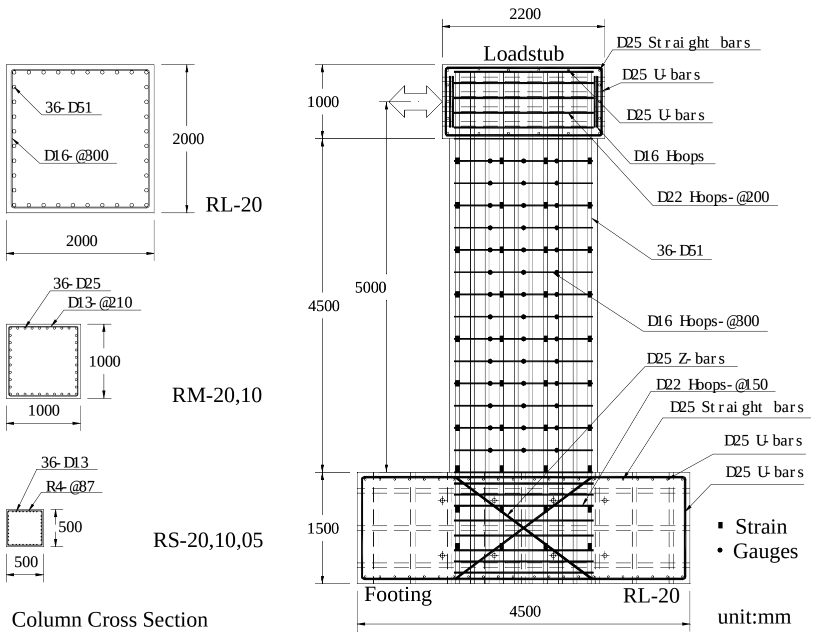

Figure 1 Reinforcement Details for test columns

Test setup and loading procedure

Details of the test setup for unit RL-20 is shown in Figure 2. Two 2940kN actuators with a maximum stroke of +/- 300mm applied the simulated horizontal seismic load. RM and RS units were also tested in single bending. No axial force was applied for RL-20. For RM and RS units, steel blocks were placed on top of each column to provide the dead load necessary to duplicate the full-scale column dead load axial stress at the column base.

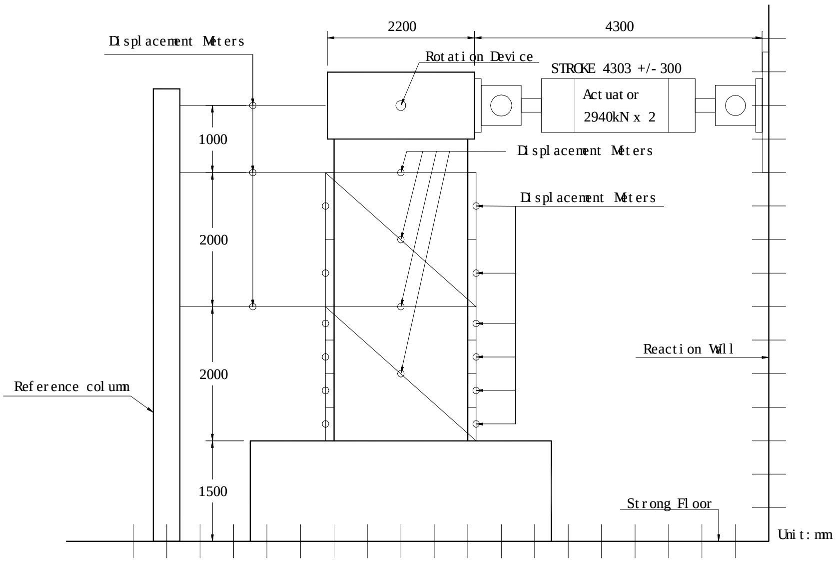

Figure 2 Column Test Setup for RL-20

The loading pattern used for the test units is shown in Figure 3. The peak of every loading cycle was controlled by force increment or the increasing displacement ductility level with three cycles at every stage. The experimental yield displacement was defined as $\Delta_y=\Delta'_y\ V_{if}/V'_y$ where V_{if} was the calculated ideal flexural strength, V'_y was the lateral force corresponding to the theoretical first yield of longitudinal reinforcement and Δ'_y was the average measured displacements at first yield in the push and pull directions. The loading sequence used for the small columns was scaled as closely as possible to follow the large column test.

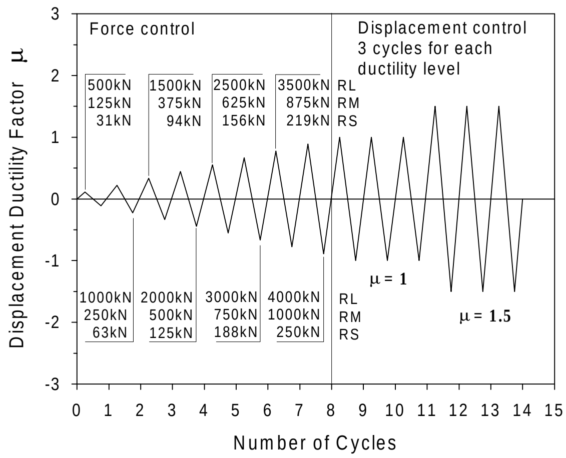

Figure 3 Loading Sequence

Lateral force applied to the specimen was measured by the load cell on the actuators. As shown in Figure 2 displacement transducers were installed diagonally, horizontally and vertically along the column height in order to compute the flexural and shear deformation of the column. Stains in the reinforcement were monitored by strain gauges mounted on the longitudinal and transverse reinforcement as shown in Figure 1.

TEST RESULTS AND DISCUSSIONS

General observations of column behavior

The overall behaviors of the small-scale units were quite similar to the full-scale specimen during testing. The experimental yield displacement of RL-20 was 42.8mm. The full-scale column and scaled models all developed shear failures just before flexural yielding except RS-10 which failed in shear at displacement ductility factors of μ_Δ=1.5 due to unexpected high compressive strength of concrete. Some of the data for RS-05 at μ_Δ=1.0 were not available because the column failed unexpectedly under force control of actuator. All other test units exhibited the similar crack propagation and showed rapid strength degradation at μ_Δ=1.0. Figure 4 shows the crack patterns of the test units at the end of the test. The critical shear crack inclinations except RL-10 were about 20 degrees to the column axis and were almost identical through the test units. However, the shear crack inclination and the maximum shear crack width at an equivalent loading stage were different between the columns. The observed shear crack inclination and the maximum crack width with the measured shear deformation are shown in Figure 5 and Figure 6 respectively. The shear crack inclination started from about 65 degrees decreased to 20 degrees for all the columns. The inclination of the larger columns reached the critical inclination at an earlier loading stage than the smaller columns, which indicated that the shear strength degradation of large columns commenced earlier than small columns. The crack width of RL-20 at μ_Δ=1.0 was 21mm which was about 4 times or 20 times of that of RM-20 and RS-20 respectively, though the shear deformation seemed to be properly scaled.

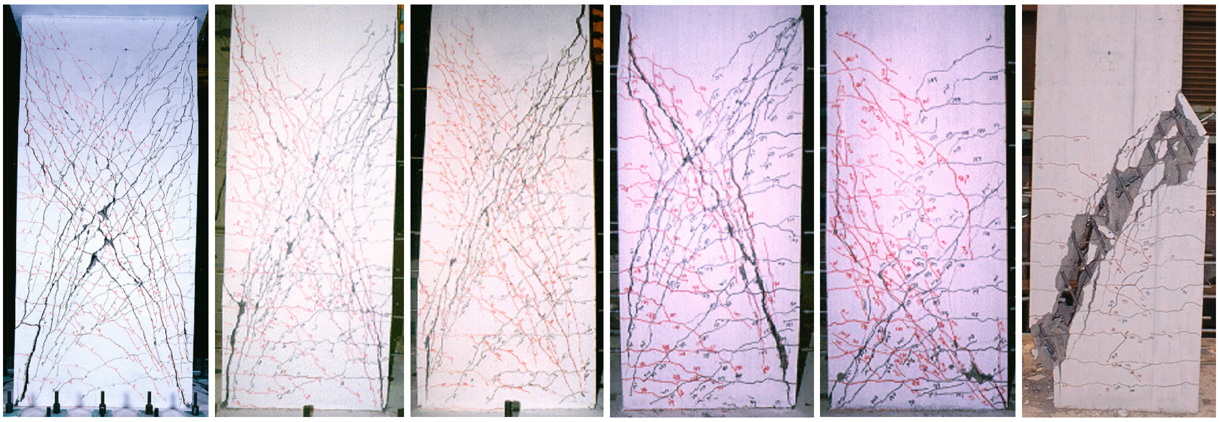

RL-20 RM-20 RM-10 RS-20 RS-10 RS-05

Figure 4 Final Crack Patterns

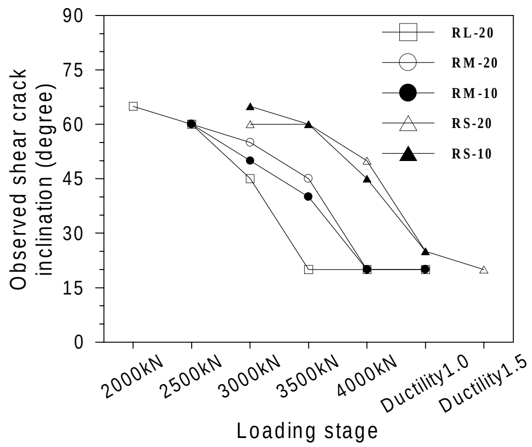

Figure 5 Observed Shear Crack Inclination

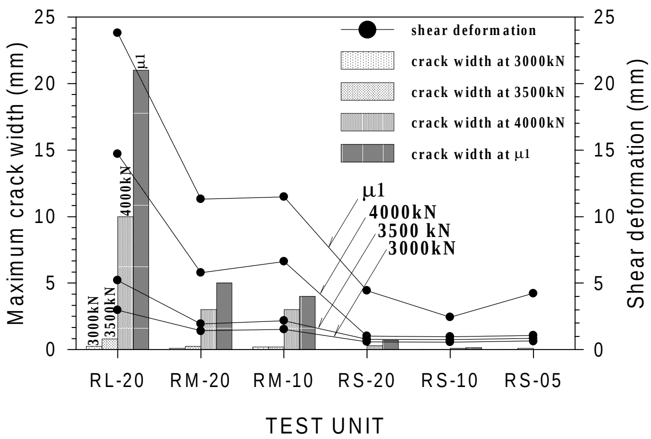

Figure 6 Observed Maximum Shear Crack Width

Force displacement responses

Figure 7 illustrates the measured lateral force-displacement hysteresis loops and the comparison of their envelopes as scaled values. The hysteresis loops are quite comparable showing the rapid strength degradation at the loading cycles of μ_Δ=1.0 except RS-10. Though the force-displacement envelopes of RL and RM units gave good agreement, RS units showed higher strengths due to high compressive strength of concrete.

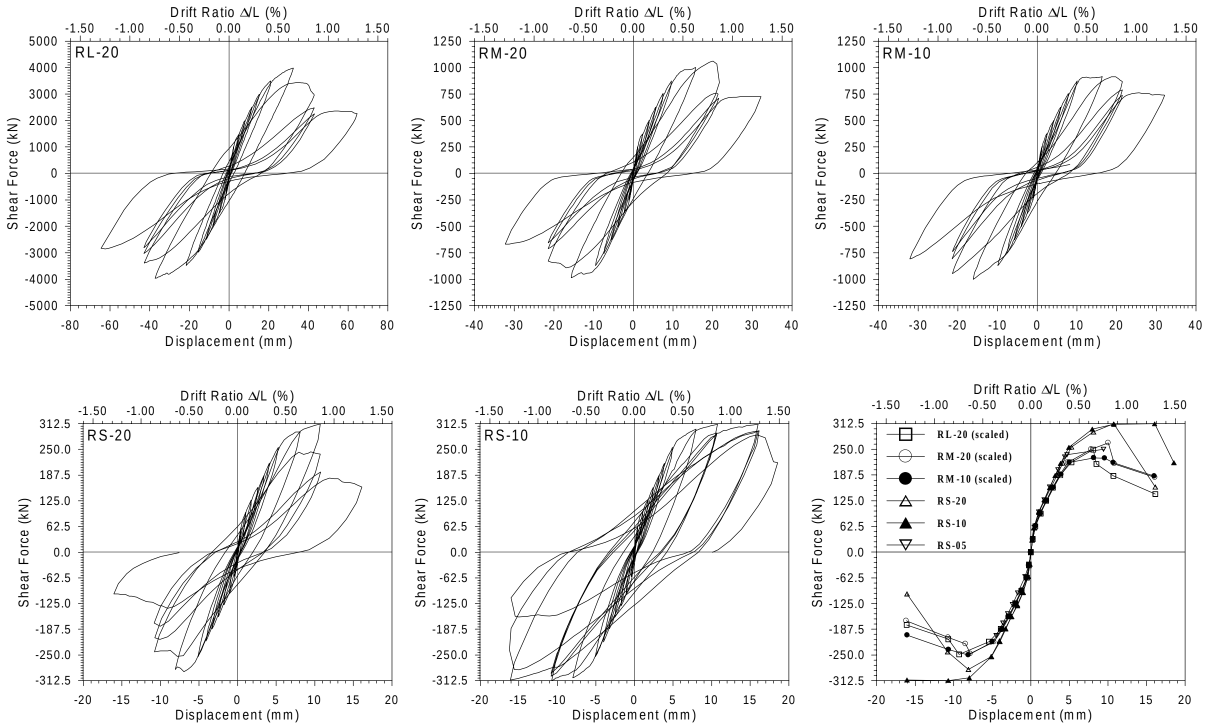

Figure 7 Hysteretic Response and Comparison of Force Displacement Envelops

The column strengths are summarised in Table 2. Also shown in the Table are calculated shear strengths of the columns based on the ACI [ACI 1995], NZS [NZS 1995] and JSCE [JSCE 1996] design codes assuming no safety factors. Although most of the calculated shear strengths are lower than the ideal flexural strengths indicating shear failure, only JSCE results gave conservative strengths to the test results. The ratios of the measured maximum strength of RM-20 and RS-20 to RL-20 were 1.07 and 1.25, and RM-10 and RS-05 were 1.00 and 0.95 respectively, which indicated the column strength increased as the column size decreased in the case of constant aggregate size. However, as shown in the calculated shear strengths, the increase of the shear strengths of RS units could also be explained as the difference of concrete strength, while JSCE gave higher ratios because of the additional scale effect coefficient.

Table 2 Strengths of Columns

Unit	*Ideal flexural strength* V_{if} (kN)	Shear strength (kN)				Ratio to RL-20			
		ACI	NZS	JSCE	Test	ACI	NZS	JSCE	Test
RL-20	5172	4454	4382	2787	3985				
scaled		278	274	174	249	1.00	1.00	1.00	1.00
RM-20	1240	1133	1115	800	1062				
scaled		283	279	200	266	1.02	1.02	1.15	1.07
RM-10	1237	1150	1132	807	1001				
scaled		288	283	202	250	1.03	1.03	1.16	1.00
RS-20	312	326	320	250	312	1.17	1.17	1.44	1.25
RS-10	313	342	335	258	312	1.23	1.22	1.48	1.25
RS-05	299	300	296	237	236	1.08	1.08	1.36	0.95

Deformation components

The disposition of displacement meters as shown in Figure 2 enabled flexural and shear components of deformation to be determined experimentally. The accuracy of these deformation components may be found by comparing the sum of both to the horizontal displacement directly measured at the top of measured segment. The comparison of the deflection components between RL-20 scaled values and RM and RS units are shown in Figure 8. The deformation components of RM units corresponded well to that of RL-20, showing constant increase of the flexural and shear deformation at low lateral load levels, and increase of the shear deformation after 3000kN where shear cracking was evident. The shear deformation exceeded the flexural one just before the shear failure and the rapid increase of the shear deflection was followed at μ_Δ=1.0 due to shear failure. The deformation components of RS-05 agreed well with RL-20, while the increase rate of the shear deformation of RS-20 was less than RL-20. This is probably because of the higher strength of concrete. The behavior of RS-10 was different from the other test units because of the different failure mode which lead to shear failure after flexural yielding at μ_Δ=1.5. The shear deformation ratio to the total displacement is shown in Figure 9. Shear accounted for approximately 17% of the total displacement at the initial loading stages, with the percentage increasing corresponding to the column degradation, and exceeded 50% at shear failure. It seemed that the deformation components were consistently scaled provided that the concrete strength was well arranged.

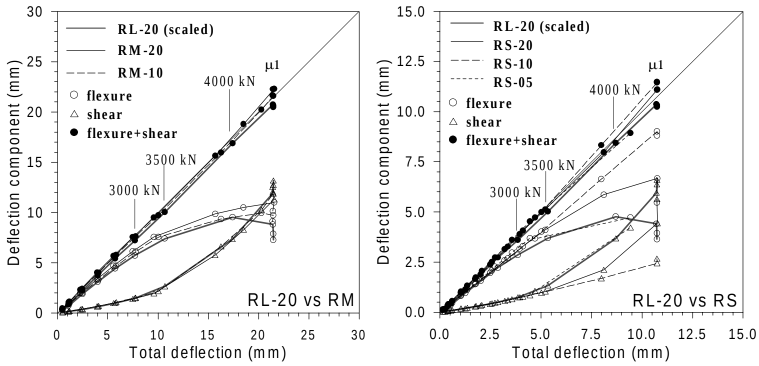

Figure 8 Deformation Components

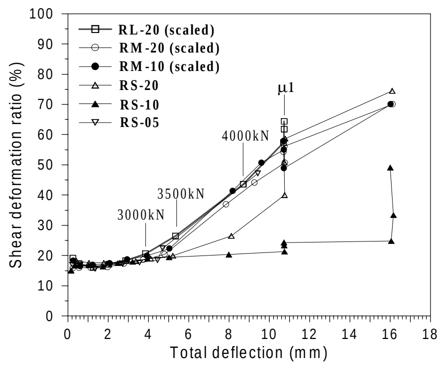

Figure 9 Shear Deformation Ratio

Concrete shear components

Shear force carried by transverse reinforcement V_s can be computed from measurements of hoop strains in the shear span as shown in Figure 1. By subtraction from the total shear, the components carried by concrete V_c could be determined. The comparison of the V_s component with force displacement envelopes and the obtained V_c component are given in Figure 10 and Figure 11 respectively. To allow comparison between column units with different concrete strengths, V_c component is expressed in the form $V_c / bd\sqrt{f'_c}$ where b and d are column width and effective depth of the section respectively and f'_c is the measured concrete compressive strength. Force and displacement of RL and RM units are consistently scaled down in the figures in order to allow the direct comparison between the test units. Figure 10 shows that the V_s component started to increase after inclined flexure-shear cracking was first observed. The increasing rate was different according to the column size corresponding to the shear cracking state as noted in Figure 5. Once V_s reached its maximum value of about V_s=110kN, it stayed constant and almost equivalent shear force V_s was obtained for all the columns as intended in the unit design. As shown in Figure 11, the maximum of total shear force and the maximum of V_c component did not occur at the same time corresponding to the strain activation of the transverse reinforcement. The degradation of the V_c component of RL-20 started at 3000kN while RM and RS degraded from 3500kN, indicating the scale effects on the V_c degradation.

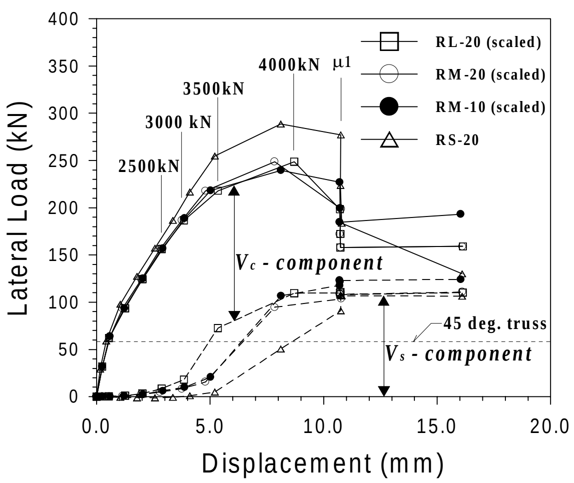

Figure 10 Hoop Shear Component

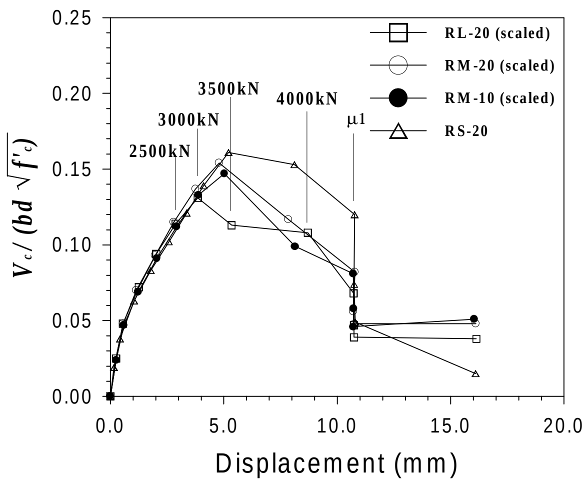

Figure 11 Concrete Shear Component

Comparison of scale effect between test results and design equations

For each column, the maximum value of concrete shear component $V_{c\text{-}max}$ and the concrete component at the maximum column strength $V_{c\text{-}column}$ versus column effective depth are plotted in Figure 12. Note that the V_c components are expressed as normalised effective shear stresses. Also shown in the figure are the effective shear stresses calculated using various design equations [ACI 1995; NZS 1995; CAN 1994; CEB-FIP 1995; JSCE 1996; JRA 1996; Bazant 1987]. It is apparent that the $V_{c\text{-}max}$ decreases with the column depth increases in both cases of constant (RL-20, RM-20, RS-20) and proportional (RL-20, RM-10, RS-05) aggregate size, indicating the shear degradation due to size effect. It should be noted that the size effect for the proportional aggregate is slightly lower than the constant aggregate size. On the other hand, though the $V_{c\text{-}column}$ gave evident scale effect when the constant aggregate size was used, $V_{c\text{-}column}$ for the proportional aggregate size seemed constant despite the column size, implying the scale effect was not significant for the maximum shear strength provided that the aggregate size was consistently scaled. The V_c component calculated from the design codes without size effect such as ACI and NZS gave unconservative prediction for large columns, while design equations with size effect seemed to appropriately estimate the V_c component yet existed substantial difference between the test and the simulated results.

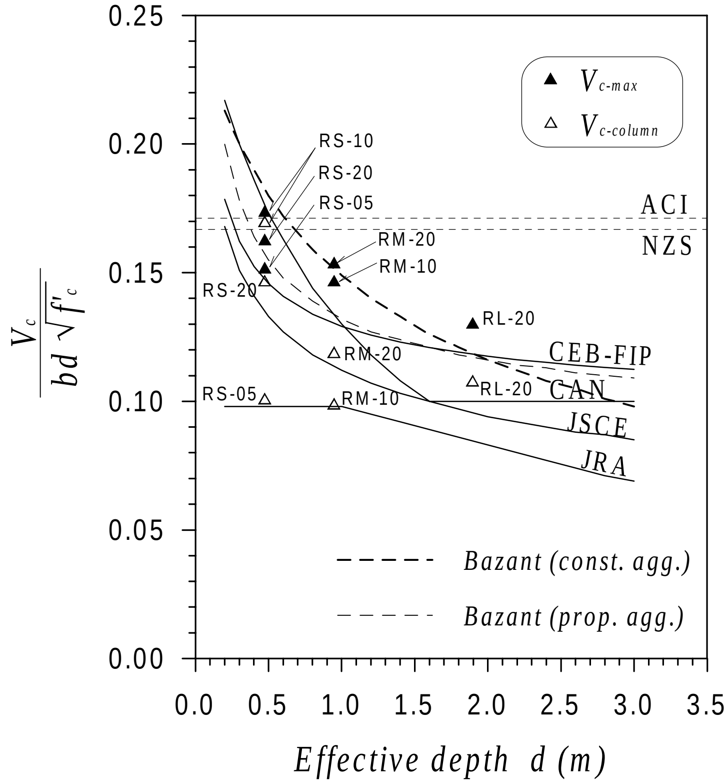

Figure 12 Size Effect on Concrete Shear Component

CONCLUSIONS

Scale effects on the shear behavior of reinforced concrete columns under seismic lateral loading were investigated through the test program using a full-scale column and scaled models. The conclusions drawn from the test results are summarised as follows:

1. The crack patterns at shear failure of the scaled models were quite similar to the full scale ones. However, the shear crack inclination and the crack width at an equivalent loading stage indicated early shear degradation of larger columns.
2. Though the force displacement responses of the test units exhibited quite comparable hysteresis loops, the difference in the maximum shear strength between the full-scale unit and the scaled models indicated the possibility of scale effects.

3. The flexural and shear deformation components seemed to be consistently scaled and hence no scale effect on the column deformation was found.
4. The activation of the V_s component of the lager columns started earlier than the smaller columns corresponding to the crack condition, which coincided with the onset of the V_c degradation.
5. Size effect on the concrete shear contribution was exhibited for the maximum V_c component in the both case of constant and proportional aggregate size while the V_c component at the maximum column strength showed the size effect only for the units with constant aggregate size.
6. Design equations that incorporate a scale factor seemed to appropriately evaluate the concrete shear contribution for reinforced concrete columns, while that without scale effect might give unconservative results for large size columns.

ACKNOWLEDGEMENT

The author would like to thank Mr. Toshiyuki KUROIWA and other research staff of the Institute of Technology, Tokyu Construction Co., Ltd., for their assistance in the experimental work of this project. The valuable suggestions on the unit design provided by Prof. M.J.N. Priestley of University of California, San Diego are very much appreciated.

REFERENCES

ACI Committee 318, “Building Code Requirements for Reinforced Concrete and Commentary,” *ACI318-95 and 318R-95*, Farmington Hills, MI., revised 1995.

ASCE-ACI Joint Task Committee 426. “Shear Strength of Reinforced Concrete Members,” *Journal of Structural Engineering*, ASCE, V.99, No.ST6, June 1973, pp.1091-1187.

Bazant, Z.P. and Sun, H.-H., “Size Effect in Diagonal Shear Failure: Influence of Aggregate Size and Stirrups,” *ACI Materials Journal Proceedings*, V.84 No.4, July-Aug. 1987, pp259-272.

Bazant, Z.P., “Fracturing Truss Model: Size Effect in Shear Failure of Reinforced Concrete,” *Journal of Engineering Mechanics*, ASCE, Dec. 1997, pp1276-1288.

Canadian Standard Association, “Design of Concrete Structures A23.3-94 Structures (Design),” Dec. 1994, 199pp.

Comite Euro-International du Beton CEB-FIP Model Code 1990, 480pp.

Collins, M. P., “The Shear Strength of Reinforced Concrete Structures”, Japan Concrete Institute Annual Convention, June 1995.

Iguro, M. Shioya, T. Nojiri, Y. and Akiyama, H., “Experimental studies on shear strength of large reinforced concrete beams under distributed load (in Japanese),” *Proceedings of JSCE No.348/V-1*, Aug. 1984, pp.175-184.

Japan Road Association, “Design Specifications of Road Bridges Part V Seismic Design (in Japanese),” Feb. 1996, 228pp.

JSCE Concrete Committee, “Standard Specification for Design and Construction of Concrete Structures, Design (in Japanese),” Japan Society of Civil Engineers, 1996, 230pp.

Kani, G.N.J., “How safe are our large concrete beams?,” *ACI Journal Proceedings*, No.64-12, 1967, pp.128-141.

McDaniel, C., Benzoni, G. and Priestley, N., "Scale Effects on the Shear Strength of Circular Reinforced Concrete Columns," University of California, San Diego, Structural Systems Laboratory, *Report No. SSRP-97/02*, August 1997.

NZS3101, “Concrete Structures Standard,” Standards Association of New Zealand, Wellington, NZ, 1995.

Ohtaki, T., Benzoni, G., and Priestley, M.J.N., "Seismic Performance of a Full Scale Bridge Column - As Built and As Repaired," University of California, San Diego, Structural Systems Laboratory, *Report No. SSRP-96/07*, November 1996, 121 pp.

Taylor, H.P.J., “Shear Strength of Large Beams,” *Journal of the Structural Division*, ASCE, Vol.98, No.ST11, November 1972, pp2473-2490.